Optical Steering of Microbubbles for Nanoparticle Transport

Arjun Krishnappa

Electrical and Computer Engineering, University of Dayton, Dayton, OH 45469

Abstract - *In this research, optical manipulation of microbubbles, and microbubbles coated with metallic nanoparticles, is investigated, both theoretically and experimentally. First, an equivalent force model on a microbubble by a focused optical beam is developed, starting from the force on a single induced dipole. This is extended to the case of microbubbles coated with metallic nanoparticles. Theoretical predictions are compared with experimental results. A focused laser beam, introduced in the vicinity of microbubbles of different sizes, attracts the microbubbles. The average velocities of these microbubbles can be related to the force imparted by the laser beam. Laser steering of the microbubbles is also experimentally demonstrated. It is shown that nanoparticles have a negligible effect on the manipulation of nanoparticle-surrounded microbubbles.*

Key Words: optics, nanotechnology, fluid dynamics, microbubbles, nanoparticles.

1. INTRODUCTION

Major applications of nanoparticles are in drug and gene delivery, bio sensing and bio imaging. The most common shape of a nanoparticle is spherical, but other shapes such as cylindrical and plate-like are also possible [1]. One of the advantages of using nanoparticles in drug delivery is the ability to deliver drugs to the specific location precisely [2][3]. A disadvantage with the traditional drug delivery system compared to the controlled drug delivery system, is that the drugs are delivered even to undesired locations [4]. Nanoparticles can be functionalized in order to have an affinity towards a specific compound, so the compounds can be easily removed by using the nanoparticles.

A review paper by Mullin *et al.* [5] discusses how microbubbles can be used to enhance nanoparticle delivery [6]. Due to the attraction between nanoparticles and microbubbles, microbubbles are surrounded by nanoparticles when they are mixed together. Thus, by loading drugs on nanoparticles, microbubbles can be used to transport these drugs from one place to other. The nanoparticle-surrounded microbubble is injected into the blood stream. Once the microbubble reaches the target cells, ultrasound is passed to break the microbubble [7][8]. This ruptures the cell membrane and easily allows the nanoparticles enter into the cells to deliver the drug.

When optical radiation is passed through a liquid, molecules in the liquid oscillate with the applied field. These oscillating molecules generate enough heat due to friction to break the molecular bonds and to change their phase from liquid to gas. This results a formation of gas microbubbles. The size of the microbubbles depends on the amount of time and radiation exposed by the liquid. It has been shown that the microbubble size increases with the laser exposure time [9]. Microbubbles can also be generated by blowing air to the liquid. One disadvantage with this method is that the microbubbles are generated with air molecules. If other molecules are required inside the microbubbles, then the respective liquid should be heated using the radiation. Thermal blooming using a focused laser beam has been used to generate microbubbles in a liquid by locally heating the liquid to its boiling point [10,11][12].

An optical device that can "trap" small particles is called an optical tweezer [13][14]. The optical tweezer is a modified microscope with a highly focused laser beam, which can generate repulsive or attractive forces [15]. Optical tweezers depend more on the gradient of the electric field because the gradient creates a force that trap particles. It requires a tight focusing laser at the sample to achieve a peak intensity gradient in order to obtain a high trapping force. Optical tweezers can be used to trap not only solid particles but also vapor microbubbles.

It has been shown by Abeywickrema and Banerjee [10] and Abeywickrema *et al.* [11] that microbubbles can be steered by using a laser [16,17]. Furthermore, there is an agglomeration of nanoparticles around the microbubble, which can be used for drug and gene delivery. The objective of this work is to study the interaction of microbubbles and nanoparticles with a focused laser beam. This research focuses on trapping microbubbles, metallic nanoparticles, and microbubbles surrounded with nanoparticles. A theoretical model for the net optical force is introduced for all the cases mentioned above and compared with experimental results.

Specifically, in Section 2, the behavior of a microbubble with a focused laser beam is analyzed theoretically by deriving the net optical force on a microbubble. Experiments with different sized microbubbles confirm that they are attracted to the center of the laser beam, and quantitative experimental results for the velocity during attraction is compared with theoretical predictions. In Section 5, the net optical force on a collection of nanoparticles is derived, and in Section 6, the analysis is extended to the case of microbubbles which have an agglomeration of nanoparticles

around it. These nanoparticle-surrounded microbubbles (NSBs) are experimentally generated and it is shown that they can also be attracted to, and steered with, the laser beam. Section 8 concludes the research work with a short description of possible future work.

2. THEORY OF OPTICAL STEERING OF MICROBUBBLES

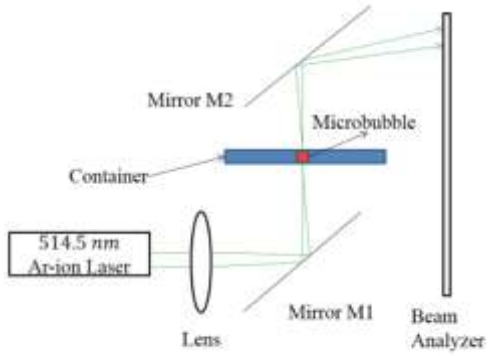

(a)

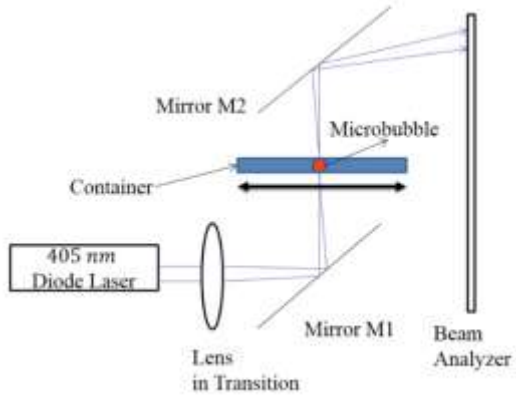

(b)

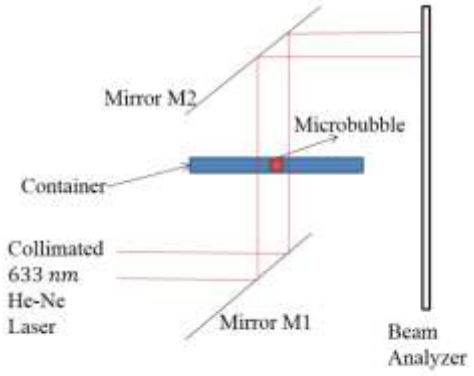

(c)

Figure 1: (a) Schematic of the generation of the microbubble due to thermal blooming by $514.5\,nm$ Ar-ion laser. (b) Steering of a microbubble along the horizontal direction by moving the lens using $405\ nm$ diode laser. (c) Monitoring the dynamics of the microbubble using the collimated $633\ nm$ He-Ne laser.

First, a $514.5\,nm$ Ar-ion laser of $50\ mW$ is used to generate the microbubble. This is done by focusing the laser beam with a lens of a focal length of $50\ cm$, onto the container [7,8] having a height of $1\ mm$ as can be seen in Figure 1(a). After the microbubble is formed, a $405\ nm$ laser of power $0.5\ mW$ is substituted for the Ar-ion laser and is used to trap and steer the microbubble. The $405\ nm$ laser is also focused using the $50\ cm$ lens and is shown in Figure 1(b). The lens is placed on a translation stage, so that the beam can be steered horizontally through the sample, by moving the lens. The $405\ nm$ laser is slowly steered towards the bubble to see the attraction of the bubble. To monitor the dynamics of the bubble, a collimated $633\ nm$, He-Ne laser of $5\ mW$ is used, as can be seen in Figure 1(c). The collimated laser beam travels through the bubble and on-axis holograms are captured using a beam profiler while the bubble is being steered using the $405\ nm$ laser beam. The microbubble is monitored until it is completely trapped by the $405\ nm$ laser. In this experiment, 100 frames are captured while the bubble is traveling to the laser beam.

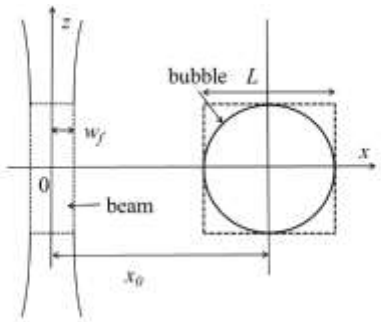

Figure 2: Schematic of steering the microbubble using optical field. The microbubble is approximated with a square of size L. The distance between the center of the Gaussian beam and the center of the microbubble is x_0. A Gaussian beam which is traveling in the z direction is focused to a waist of W_f at $z = 0$.

Figure 2 shows a schematic of steering a microbubble using an optical field which is used to derive the general force model. A microbubble with a diameter of L and a Gaussian beam with a waist of W_f (focused at $z = 0$) are considered. Laser beam is assumed to be propagating along the z-axis, and the distance between the centers of the bubble and the

beam is x_0. Note that the shape of the microbubble is assumed to be a cube with side length of L for simplicity. Also, the calculated Rayleigh range of the Gaussian beam is much larger than the dimensions of the microbubble. So, the beam can be considered as a collimated beam throughout the derivation and calculations. The net force exerted by the laser on the microbubble can be calculated by summing all forces due to each and every molecule inside the microbubble.

Intensity profile of a collimated Gaussian beam of waist W_f in x dimension can be expressed as,

$$I(x) = I_0 \exp\left(-\frac{x^2}{W_f^2}\right), \quad (1)$$

where I_0 is the peak intensity of the Gaussian beam. The relation between the intensity and electric field is given by,

$$I(x) = \frac{c n_l \epsilon_0}{2} |E_e(x)|^2, \quad (2)$$

where c is the velocity of light in vacuum, n_l is the refractive index of the liquid, and ϵ_0 is the free-space permittivity. Then the force on an induced dipole within the microbubble in x direction can be calculated using the following equation,

$$F(x)_{dipole} = \left(\frac{\alpha}{4}\right)\frac{2}{c n_l \epsilon_0} I_0 \frac{\partial}{\partial x}\left(\exp\left(-\frac{x^2}{W_f^2}\right)\right). \quad (3)$$

Net force, F_{BI} on a microbubble that consists of induced dipoles can be then obtained by integrating Eq. (3) over the dimensions of the microbubble as,

$$F_{BI} = N L^2 \left(\frac{\alpha}{4}\right)\frac{2}{c n_l \epsilon_0} I_0 \int_{(x_0-\frac{L}{2})}^{(x_0+\frac{L}{2})} \frac{\partial}{\partial x}\left(\exp\left(-\frac{x^2}{W_f^2}\right)\right) dx, \quad (4)$$

where N is the number of dipoles per unit volume. Then the net force on the microbubble after the integration can be obtained as,

$$F_{BI} = -\frac{N L^2 \alpha}{c n_l \epsilon_0} I_0 \exp\left(-\frac{x_0^2 + \left(\frac{L}{2}\right)^2}{W_f^2}\right) \sinh\left(\frac{x_0 L}{W_f^2}\right). \quad (5)$$

Furthermore, the total polarizability of N dipoles can be expressed in terms of the relative permittivity, ϵ_{rv} and the permittivity of free space, ϵ_0 assuming each dipole has a polarizability of α as,

$$N\alpha = \epsilon_0(\epsilon_{rv} - 1). \quad (6)$$

Substituting Eq. (6) in to Eq. (5) the final force equation reduces to

$$F_{BI} = -L^2 \frac{(\epsilon_{rv}-1)}{c n_l} I_0 \exp\left(-\frac{x_0^2 + \left(\frac{L}{2}\right)^2}{W_f^2}\right) \sinh\left(\frac{x_0 L}{W_f^2}\right). \quad (7)$$

3. SIMULATION RESULTS

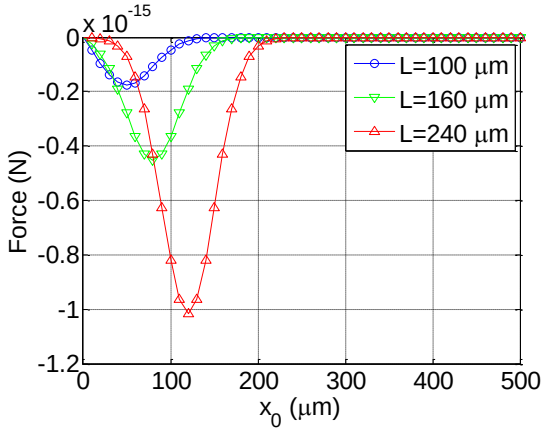

Figure 3: Variation of the net optical force with x_0 on a $100\ \mu m$ (blue), $160\ \mu m$ (green), $240\ \mu m$ (red) microbubble.

Figure 3 shows a typical plot of the net force, F_{BI} as a function of the separation, x_0 between the microbubble and the beam. Simulations are performed for three different sizes of microbubbles, $100\ \mu m$, $160\ \mu m$, and $240\ \mu m$. A $405\ nm$ laser with a power $P = 0.5\ mW$ focused down to a waist size of $W_f \approx 42\ \mu m$ is used for the simulation. Values of n_l and ϵ_{rv} are 1.4 and 1.0005, respectively. Calculated $N\alpha$ using above values is $3 \times 10^{-15}\ F m^{-1}$. The peak intensity is calculated according to the relation, $I_0 = \frac{P}{\pi W_f^2}$ and found to be in the order of $10^5\ W m^{-2}$. Isopropanol liquid is used to generate microbubbles by heating with the laser beam.

As can be seen the x-component force in Figure 3 the maximum force increases as the size of the microbubble increases. Also, it is observed that the value of x_0 corresponds to the maximum force increases with the microbubble size. The x-component force appears due to the gradient of the electric field intensity of light and is commonly referred as gradient force. This force component completely vanishes at the center of the beam thus trapping the microbubbles at that position. Larger microbubbles contain more dipoles compared to smaller microbubbles. Larger microbubbles take place because the isopropanol liquid is heated more compared to the smaller microbubbles. The more the isopropanol liquid is heated, the more the dipoles are formed. Thus, larger microbubbles should have a higher induced force than smaller microbubbles, which is also explained from the simulation results.

The velocity $v = dx_0/dt$ of the microbubble can be found by solving the differential equation

$$F_{Bl} = -L^2 \frac{(\epsilon_{rv}-1)}{cn_l} I_0 \exp\left(-\frac{x_0^2+\left(\frac{L}{2}\right)^2}{W_f^2}\right) \sinh\left(\frac{x_0 L}{W_f^2}\right) = m_v dv/dt = m_v d^2x_0/dt^2 \quad (8)$$

where m_v is the mass of the microbubble. In order to find the exact velocity Eq. (10) should be numerically integrated. In this case an approximate value for the velocity is calculated as follows. The density ρ_v of the gas inside the microbubble is taken to be approximately $1 kg/m^3$ which is close to air. So for a microbubble with a diameter of $100 \mu m$, the mass m_v is approximately $10^{-12} kg$. Assuming a peak force of $10^{-15} N$, the acceleration, dv/dt of the microbubble can be calculated as in the order of $10^{-3} m/s^2$. This means that the velocity of the microbubble is up to $1 mm/s$ for a $1\ s$. Note that the above velocity is calculated assuming a cubic microbubble. This has to be converted to the case of a spherical microbubble to obtain the exact velocity. It is understood that a volume integration should be performed to obtain an accurate value for the force. In this case the conversion factor is obtained by squaring the ratio of the volumes of a sphere and cube with identical dimensions. Calculated conversion factor, C approximately is $\left(\frac{\pi}{6}\right)^2 \approx 0.25$ [18]. Hence the velocity for a sphere can be determined by multiplying the velocity of the cube by conversion factor, which yields about $250\ \mu m/s$. This is in good agreement with the measured values of the average velocity as can be seen in the experimental section. The deviation between the results obtained experimentally and theoretically is very small, which arises because of measurement errors. The spherical microbubbles are assumed to be cubes, but by the conversion factor the calculated net force on the particles in the cubes can be precisely converted to the net force on the particles in the spherical microbubbles.

4. EXPERIMENTS

In this experiment, 100 frames are captured while the bubble is being steered towards the laser until it traps. Only six frames of the whole process are shown in Figure 4.

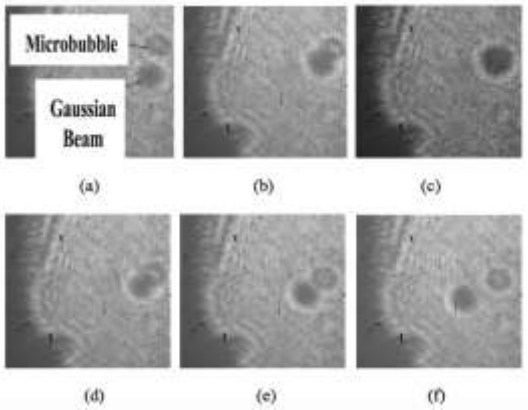

Figure 4: In-line holograms of the microbubble along with the laser spot recorded with a CCD array. (a) through (c) shows how the microbubble is attracted towards the center of the beam. (d) through (f) shows how the microbubble can be separated from the beam.

Recorded images can be used to calculate the average velocity of the microbubble by knowing the frame rate and distance between the bubble and the laser beam. The distance between the microbubble and the laser beam can be approximately calculated by multiplying the number of pixels between centers of the microbubble and the beam and pixel size. Table 1 shows the experimental average velocities for three different sizes of microbubbles, $100\ \mu m$, $160\ \mu m$, and $240\ \mu m$. From the experiment it is observed that the smaller microbubbles have a slightly lower average velocity than the larger microbubbles. It is also observed that the small microbubbles need relatively less force to separate from the laser beam compared to the larger microbubbles, which is because of the reason that smaller microbubbles have lesser number of dipoles than the larger microbubbles.

Table 1: Experimental determination of average velocity for different sized microbubbles under laser trapping.

Microbubble size $L\ (\mu m)$	100	160	240
Separation x_0	150	180	220
Time of travel (s)	1.65	1.92	2.24
Average velocity $(\mu m/s)$	91	93	98

5. THEORY FOR THE BEHAVIOR OF NANOPARTICLES IN THE PRESENCE OF AN OPTICAL FIELD

In this section, a force model is introduced to explain the behavior of a cluster of nanoparticles when they reside on a surface of a hypothetical empty cube with a negligible mass. Figure 5 shows a two-dimensional view of a schematic of steering the nanoparticle-surrounded empty cube of side

length L. A Gaussian beam with a waist of W_f (focused at $z = 0$) is assumed to be propagating along the z-axis, and its center is at a distance of x_0 from the center of the empty cube. The net force on the cube is the sum of the forces induced in each nanoparticle. Here, silver nanoparticles are considered and the wavelength is considered as 405 nm because 20 nm silver nanoparticles have the maximum absorbance around this wavelength.

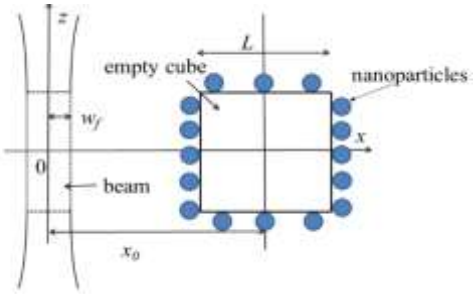

Figure 5: Schematic of steering the nanoparticles using a focused laser beam. Distance between the center of the Gaussian beam and the center of the empty cube is x_0. A Gaussian beam which is traveling in the z direction is focused to a waist of W_f at $z = 0$. A 405nm diode laser with a power of 0.5mW is used as the source and silver nanoparticles are considered.

Using Eq. (3), the force F_{NPI} on an induced dipole as in the case of a nanoparticle can be written as

$$F_{NPI} = \left(\frac{\alpha_N}{4}\right)\frac{2}{cn\epsilon_0} I_0 \nabla\left(\exp\left(-\frac{x^2}{W_f^2}\right)\right), \quad (9)$$

with

$$\alpha_N = \frac{4\pi r^3(\epsilon_i(\omega)-\epsilon_h)4\pi\epsilon_0}{(\epsilon_i(\omega)+2\epsilon_h)10^{12}}, \quad (10)$$

where ϵ_i and ϵ_h are the relative permittivity of the nanoparticle and the relative permittivity of the surrounding liquid, respectively, ω is the frequency and r is the radius of the nanoparticle. The units of α_N in Eq. (10) is Fm^2. Equation (9) can be simplified to

$$F_{NPI} = -\frac{\alpha_N}{4}\frac{2}{cn\epsilon_0} I_0 \left(\frac{2x}{W_f^2}\right)\exp\left(-\frac{x^2}{W_f^2}\right). \quad (11)$$

The net force F_{NPCI} on the nanoparticle cluster around the hypothetical volume can be calculated by summing all the forces from each side of the cube and can be expressed as

$$F_{NPCI} = F_{NPCI}\left(-\frac{L}{2}\right) + 4F_{NPCI}\left(-\frac{L}{2} < x < \frac{L}{2}\right) + F_{NPCI}\left(\frac{L}{2}\right), \quad (12)$$

where $F_{NPCI}(-\frac{L}{2})$ and $F_{NPCI}(\frac{L}{2})$ are the forces on the left and right sides of the cube at $x = x_0 - \frac{L}{2}$ and $x = x_0 + \frac{L}{2}$, respectively, of the cube, which can be calculated by substituting $x = x_0 - \frac{L}{2}$ and $x = x_0 + \frac{L}{2}$ in Eq. (11), respectively and written as

$$F_{NPCI}\left(-\frac{L}{2}\right) = -N''\,L^2\,\frac{\alpha_N}{4}\frac{2}{cn\epsilon_0} I_0\left(\frac{2\left(x_0-\frac{L}{2}\right)}{W_f^2}\right)\exp\left(-\frac{\left(x_0-\frac{L}{2}\right)^2}{W_f^2}\right), \quad (13)$$

and

$$F_{NPCI}\left(\frac{L}{2}\right) = -N''\,L^2\,\frac{\alpha_N}{4}\frac{2}{cn\epsilon_0} I_0\left(\frac{2\left(x_0+\frac{L}{2}\right)}{W_f^2}\right)\exp\left(-\frac{\left(x_0+\frac{L}{2}\right)^2}{W_f^2}\right), \quad (14)$$

where N'' is the number of nanoparticles per unit area and $N''L^2$ gives the number of nanoparticles on one side of the cube.

The net force $F_{NPCI}(-\frac{L}{2} < x < \frac{L}{2})$ on nanoparticles on the 4 sides where x varies from $x_0 - \frac{L}{2}$ to $x_0 + \frac{L}{2}$, can be calculated using Eq. (4) as

$$F_{NPCI}\left(-\frac{L}{2} < x < \frac{L}{2}\right) = N''L\left(\frac{\alpha_N}{4}\right)\frac{2}{cn\epsilon_0} I_0 \int_{(x_0-\frac{L}{2})}^{(x_0+\frac{L}{2})}\frac{\partial}{\partial x}\left(\exp\left(-\frac{x^2}{W_f^2}\right)\right)dx \quad (15)$$

After integrating the total force on all the nanoparticles from $x = x_0 - \frac{L}{2}$ to $x = x_0 + \frac{L}{2}$ can be written as

$$F_{NPCI}\left(-\frac{L}{2} < x < \frac{L}{2}\right) = -2N''L\frac{\alpha_N}{4}\frac{2}{cn\epsilon_0} I_0 \exp\left(-\frac{x_0^2+\left(\frac{L}{2}\right)^2}{w_f^2}\right)\sinh\left(\frac{x_0 L}{w_f^2}\right) \quad (16)$$

After substituting Eqs. (13), (14), and (16) in Eq. (12), the net force can be calculated as

$$\begin{aligned} F_{NPCI} = {} & -N''\,L^2\,\frac{\alpha_N}{4}\frac{2}{cn\epsilon_0} I_0\left(\frac{2\left(x_0-\frac{L}{2}\right)}{W_f^2}\right)\exp\left(-\frac{\left(x_0-\frac{L}{2}\right)^2}{W_f^2}\right) \\ & -8N''L\frac{\alpha_N}{4}\frac{2}{cn\epsilon_0} I_0\exp\left(-\frac{x_0^2+\left(\frac{L}{2}\right)^2}{W_f^2}\right)\sinh\left(\frac{x_0 L}{W_f^2}\right), \\ & -N''\,L^2\,\frac{\alpha_N}{4}\frac{2}{cn\epsilon_0} I_0\left(\frac{2\left(x_0+\frac{L}{2}\right)}{W_f^2}\right)\exp\left(-\frac{\left(x_0+\frac{L}{2}\right)^2}{W_f^2}\right) \end{aligned} \quad (17)$$

which can be further simplified as

$$F_{NPCI} = -L\alpha_N \frac{2}{cn\epsilon_0} I_0 \left\{ 2N'' \exp\left(-\frac{x_0^2+\left(\frac{L}{2}\right)^2}{W_f^2}\right) \sinh\left(\frac{x_0 L}{W_f^2}\right) + \frac{N''\ L}{2W_f^2}\left[\left(x_0 - \frac{L}{2}\right)\exp\left(-\frac{\left(x_0-\frac{L}{2}\right)^2}{W_f^2}\right) + \left(x_0 + \frac{L}{2}\right)\exp\left(-\frac{\left(x_0+\frac{L}{2}\right)^2}{W_f^2}\right)\right]\right\} \quad (18)$$

6. THEORY FOR OPTICAL STEERING OF NANOPARTICLE-SURROUNDED MICROBUBBLES USING A FOCUSED LASER BEAM

A temperature gradient and convective flow are formed around a microbubble when the microbubble is generated using a focused laser beam. When nanoparticles are in the vicinity of the microbubble, they can be attracted to the microbubble along the bottom surface due to the convective flow. Once particles reach the microbubble, they get attached to the surface of the microbubble [19].

Steering of NSBs can be modeled by combining the models in section 2 and 5 and shown in Figure 6. A Gaussian beam is assumed to be propagating along the z axis with a beam waist of W_f is considered. The NSB is considered as a cube of side length L instead of a sphere for simplicity. The beam is considered to be collimated assuming that the Rayleigh range is much larger than the size of the NSB. The net force on the NSB is the sum of the total force on all the nanoparticles and the force on all the molecules inside the microbubble. In this section a general force model is introduced to explain the behavior of a NSB in the presence of a focused laser beam.

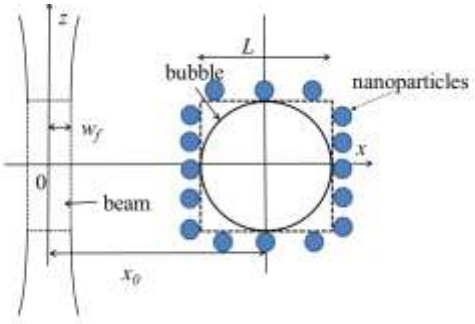

Figure 6: Schematic of steering a NSB using a focused laser beam. Distance between the center of the Gaussian beam and the center of the microbubble is x_0. A Gaussian beam which is traveling in the z direction is focused to a waist of W_f at $z = 0$. A 405 nm diode laser with a power of 0.5 mW is used as the source and silver nanoparticles are considered.

The net force on a NSB can be expressed by combining the force equations Eq. (7) and Eq. (18) as

$$F_{NSBI} = F_{BI} + F_{NPCI}, \quad (19)$$

where F_{BI} and F_{NPCI} are the net forces on a microbubble and nanoparticle clusters, respectively. By substituting the respective forces which are calculated in section 2 and 5, the total force can be calculated as,

$$F_{NSBI} = -2NL^2 \frac{\alpha}{4}\frac{2}{cn\epsilon_0} I_0 \exp\left(-\frac{x_0^2+\left(\frac{L}{2}\right)^2}{W_f^2}\right)\sinh\left(\frac{x_0 L}{W_f^2}\right) - L\alpha_N \frac{2}{cn\epsilon_0} I_0 \left\{ 2N'' \exp\left(-\frac{x_0^2+\left(\frac{L}{2}\right)^2}{W_f^2}\right)\sinh\left(\frac{x_0 L}{W_f^2}\right) + \frac{N''\ L}{2W_f^2}\left[\left(x_0 - \frac{L}{2}\right)\exp\left(-\frac{\left(x_0-\frac{L}{2}\right)^2}{W_f^2}\right) + \left(x_0 + \frac{L}{2}\right)\exp\left(-\frac{\left(x_0+\frac{L}{2}\right)^2}{W_f^2}\right)\right]\right\} \quad (20)$$

7. EXPERIMENTS

An experiment is performed to verify the theoretical results observed in the previous Section. A naturally generated microbubble in a mixture of silver nanoparticles, isopropanol and red dye is steered using a 405 nm diode laser. Images are captured using the same techniques mentioned in Section 2 and the microbubble size is calculated to be about 80 μm. Figure 7(a) shows the position where the microbubble starts to move towards the laser beam. Figure 7(b) is an image when the microbubble is completely trapped by the laser beam. At this point both the microbubble and the beam are on top of each other. The average velocity is calculated using the distance traveled by microbubble and the time, as mentioned in Section 3. The estimated time to move a distance of 140 μm, which is the distance between the center of the beam and the microbubble is 1.6 s, which yields an average velocity of about 88 $\mu m/s$.

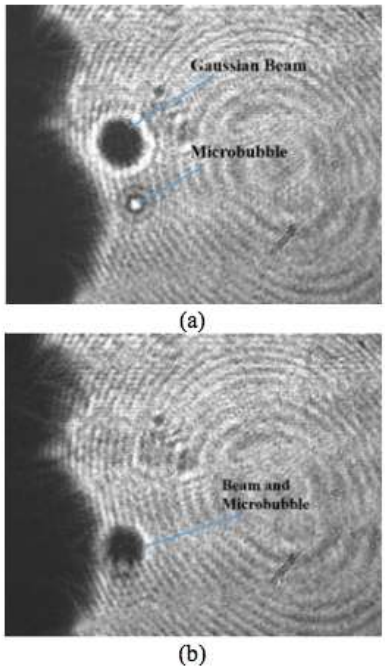

Figure 7: Images of two stages when a microbubble is trapped by a focused laser beam. (a) The beam at a distance of $140\ \mu m$ from a $80\ \mu m$ NSB. (b) Trapping of the $80\ \mu m$ NSB at the center of the beam. Both the beam and the microbubble are on top of each other at this point.

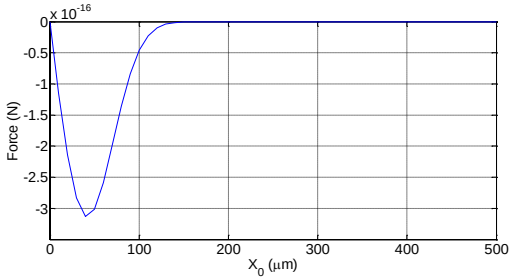

Figure 8: Variation of the theoretically calculated optical force with x_0 for a $80\ \mu m$ NSB.

Figure 8 shows the theoretically calculated optical force on a $80\ \mu m$ NSB as a function of the separation between the beam and the microbubble. The experimentally measured average velocity for the $80\ \mu m$ NSB is found to be about $88\ \mu m/s$ as mentioned earlier. The theoretical acceleration, following the procedure in Section 2, is found to be $75\ \mu m/s^2$. Thus in $1\ s$, the expected velocity is up to $75\ \mu m/s$, which is in good agreement with the experimental value mentioned above.

8. CONCLUSION

In this work, the behavior of microbubbles in the presence of a focused laser beam is studied in detail. A force model is introduced to calculate the induced force on a microbubble due to an optical field. Simulations are done to determine the net force on the microbubble using MATLAB®. Experiments are also performed to confirm the theoretical results using different sizes of microbubbles. It is shown that the experimental results are in good agreement with the theoretical predictions of the "trapping" velocities. It is observed that the smaller microbubbles move with a low velocity compared to larger microbubbles. Thus, to steer with a same velocity, small microbubbles require more laser power. Also, it is observed that the small microbubbles can be easily separated from the laser beam compared to larger microbubbles. This model is derived assuming the microbubble to be a cube, not a sphere. As mentioned earlier a volume integral should be performed in order to obtain an accurate value for the force and the velocity which can be considered as future work. Also, a force model for the case when the microbubble is surrounded by metallic nanoparticles is derived in this paper.

REFERENCES

[1] Y. Liu, J. Tan, A. Thomas, D. Ou-yang, and V. Muzyknotav, "The shape of things to come: Importance of design in nanotechnology for drug delivery," Therapy Delivery **3**, 181-194 (2012).

[2] S. Mudshinge, A. Deore, S. Patil, and C. Bhalgat, "Nanoparticles: emerging carriers for drug delivery," Saudi Pharm. Jour. **19**, 129-141 (2011).

[3] J. Patra, G. Das, and L. Fraceto, "Nano based drug delivery systems: recent developments and future prospects," J. Nanobiotechnology **16**, (2018).

[4] Z. Doswiadczalnej, U. Kanska, R. Budzynska, and J. Boratynski, "Current status of research on conjugates and related drug delivery systems in the treatment of cancer and other diseases," Postepy Higieny Medycyny Doswiadczainej **61**, 350–360 (2007).

[5] L. Mullin, L. Phillips, and P. Dayton, "Nanoparticle delivery enhancement with acoustically activated Microbubbles," IEEE Trans. Ultrasonics, Ferroelectrics and Frequency Control **60**, 65-77(2013).

[6] R. Browning and E. Stride, "Microbubble-mediated delivery for cancer therapy," Fluids **3**, 1-12 (2018).

[7] S. Hernot and A. Klibanov, "Microbubbles in ultrasound-triggered drug and gene delivery," Adv. Drug Delivery Rev. **60**, 1153-1166 (2008).

[8] J. Owen, C. Crake, J. Lee, D. Carugo, E. Beguin, A. Khrapitchev, R. Browning, N. Sibson, and E. Stride, "A versatile method for the preparation of particle-loaded microbubbles for multimodality imaging and targeted drug delivery," Drug Deliv Transl Res. **8**, 342-356 (2018).

[9] D. Lapotko, "Plasmonic nano microbubbles as tunable cellular probes for cancer theranostics," J. Cancers **3**, 802-840 (2011).
[10] U. Abeywickrema and N. Banerjee, "Characterization and application of Microbubbles during thermal blooming," Proc. SPIE **9194**, 91940H 1-7 (2014).
[11] U. Abeywickrema, P. Banerjee, and N. Banerjee, "Holographic assessment of self-phase modulation and blooming in a thermal medium," Appl. Opt. **54**, 2857-2865 (2015).
[12] U. Abeywickrema, C. Zhao, and P. Banerjee, "Dynamics of thermally generated micro bubbles," Proc. SPIE **10520**, 105201S 1-6 (2018).
[13] A. Ranaweera, "Investigations with optical tweezers: construction, identification, and control," Dissertation, U. California Santa Barbara (2004).
[14] J. Liu and Z. Li, "Controlled mechanical motions of microparticles in optical tweezers," Micromachines **9**, 1-5 (2018).
[15] K. Neuman and S. Block, "Optical trapping," Rev. Sci. Instrum. **75**, 2787-2809 (2004).
[16] A. Krishnappa, U. Abeywickrema, and P. Banerjee, "Optical steering of thermally generated microbubbles in a liquid for targeted metallic nanoparticle delivery," Proc. SPIE **9922**, 99222V 1-7 (2016).
[17] A. Krishnappa, "Optical steering of microbubbles for nanoparticle transport," Thesis, University of Dayton (2016).
[18] A. Krishnappa, "Laws of nature for forces: the discovery of cubal laws and constant," Proc. SPIE **10106**, 101061W 1-12 (2017).
[19] C. Zhao, Y. Xie, Z. Mao, Y. Zhao, J. Rufo, S. Yang, F. Guo, D. Mai, and T. Huang, "Theory and experiment on particle trapping and manipulation via optothermally generated microbubbles," J. Lab Chip **14**, 384-391 (2014).